Alectinib Resistance in ALK-rearranged Lung Cancer by Dual Salvage Signaling in a Clinically Paired Resistance Model

Authors: Takahiro Tsuji[1], Hiroaki Ozasa[1]*, Wataru Aoki[2], Shunsuke Aburaya[2], Tomoko Funazo[1], Koh Furugaki[3], Yasushi Yoshimura[3], Hitomi Ajimizu[1], Ryoko Okutani[1], Yuto Yasuda[1], Takashi Nomizo[1], Kiyoshi Uemasu[1], Koichi Hasegawa[1], Hironori Yoshida[1], Yoshitaka Yagi[1], Hiroki Nagai[1], Yuichi Sakamori[1], Mitsuyoshi Ueda[2], Toyohiro Hirai[1], and Young Hak Kim[1]

Affiliations:

[1] Department of Respiratory Medicine, Kyoto University Graduate School of Medicine, Kyoto, Japan.

[2] Division of Applied Life Sciences, Graduate School of Agriculture, Kyoto University, Kyoto, Japan.

[3] Product Research Department, Kamakura Research Laboratories, Chugai Pharmaceutical, Kanagawa, Japan.

Running title:

Clinical Paired Cell Model System of Alectinib Resistance

Additional information:

Financial support: Grant support: Takahiro Tsuji is supported by a Research Fellowship for Young Scientists by the Japan Society for the Promotion of Science (Project No: 16J03807). This work and Hiroaki Ozasa are supported by Chugai Pharmaceutical Co., Ltd. (Tokyo, Japan).

***To whom correspondence should be addressed:**

Hiroaki Ozasa, M.D., Ph.D.

Department of Respiratory Medicine, Kyoto University Graduate School of Medicine. 54, Shogoin-kawaharacho, Sakyo-ku, Kyoto 606-8507, Japan.

Telephone: +81-75-751-3830 Fax: +81-75-751-4643

E-mail: ozahiro@kuhp.kyoto-u.ac.jp

Potential conflict of interests: Toyohiro Hirai is supported by Chugai Pharmaceutical Co., Ltd. Young Hak Kim is supported by Chugai Pharmaceutical Co.,Ltd., AstraZeneca K.K. (Osaka, Japan), Ono Pharmaceutical Co.,Ltd. (Osaka, Japan), Bristol-Myers Squibb K.K. (Tokyo, Japan), Boehringer Ingelheim Japan, Inc. (Tokyo, Japan), and Eli Lilly Japan K.K (Kobe, Japan) as a honorarium recipient.

Other notes:

Word count: words: 5002

Total number of figures: 7 (Number of color figures: 4)

Abstract

The mechanisms responsible for the development of resistance to alectinib, a second-generation anaplastic lymphoma kinase (ALK) inhibitor, are still unclear and few cell lines are currently available for investigating ALK-rearranged lung cancer. To identify the mechanisms underlying acquired resistance to alectinib, two patient-derived cell lines were established from an alectinib-naïve ALK-rearranged lung cancer and then after development of alectinib resistance. The properties acquired during treatments were detected by comparisons of the two cell lines, and then functional analyses were performed. Co-activation of c-Src and MET were identified after the development of alectinib resistance. Combinatorial therapy against Src and MET significantly restored alectinib sensitivity in vitro (17.2-fold). Increased apoptosis, reduction of tumor volume, and inhibition of MAPK and PI3K/AKT signaling molecules for proliferation and survival were observed when the three kinases (Src, MET, and ALK) were inhibited. A patient-derived xenograft from the alectinib-resistant cells indicated that combination therapy with a saracatinib and crizotinib significantly decreased tumor size in vivo. To confirm the generality, a conventional alectinib-resistant cell line model (H2228-AR1S) was established from NCI-H2228 cells (EML4-ALK variant 3a/b). In H2228-AR1S, combination inhibition of Src and MET also restored alectinib sensitivity. These data reveal that dual salvage signaling from MET and Src is a potential therapeutic target in alectinib-resistant patients.

Implication: This study demonstrates the feasibility to elucidate personalized drug-resistance mechanisms from individual patient samples.

Introduction

The discovery of driver oncogenes and development of targeted therapy have contributed to improved prognoses in patients with non-small cell lung cancer (NSCLC). (1,2) In 2007, a novel driver oncogene, the echinoderm microtubule-associated protein-like 4 and anaplastic lymphoma kinase (*EML4-ALK*) fusion caused by chromosomal rearrangements was identified in patients with NSCLC (3) and its first-generation targeted therapy, crizotinib became the standard first-line therapy for patients with ALK-rearranged NSCLC. (4) Although crizotinib improved median progression-free survival (PFS) over that with conventional chemotherapy (10.9 vs 7.0 months; HR 0.45: 95% CI 0.35-0.60) (5) tumors relapsed due to the acquisition of resistance. Secondary mutations, such as L1196M, C1156Y, and G1202R, occur in the kinase domain of ALK, and decrease the affinity of crizotinib to ALK and maintain EML4-ALK activity. (6-8) Salvage signaling pathways, such as epidermal growth factor receptor (EGFR) and KIT, maintain downstream proliferation and survival signaling, such as PI3K/Akt or MAPK, independent of the ALK-fusion protein, which promotes growth and survival if oncogenic ALK signaling is inhibited. (8,9) Secondary mutations have been implicated as frequent causes of ALK inhibitor resistance than salvage signaling, and one possible explanation for this is that crizotinib exhibits relatively low affinity to ALK and targets multiple tyrosine kinases, such as c-MET and ROS1.

The second generation ALK inhibitors, alectinib and ceritinib, which exhibit higher specificities and affinities to ALK than crizotinib, (10) may inhibit several secondary-mutated ALKs and achieve promising clinical efficacies in crizotinib-resistant patients and ALK-inhibitor naïve patients. (11-13) However, tumors also eventually relapse. Based on this high specificity and affinity to ALK, some researchers hypothesized that the frequency and number of gatekeeper mutations may be limited and that more bypass signals may occur during treatments with second generation ALK inhibitors. (14) Few studies have investigated the mechanisms responsible for the development of alectinib resistance, and the extensive evidence obtained for acquired resistance to crizotinib may not be applicable to alectinib.

The establishment of drug-resistant tumor models has contributed to the elucidation of novel mechanisms for acquired drug resistance. (14,15) However, ALK-rearranged NSCLC are relatively rare (5% of NSCLC) and few cell line models are currently available for investigating ALK-rearranged lung cancer; (16) only one cell line is presently offered on a commercial basis. To clarify the mechanisms underlying the development of alectinib resistance in ALK-rearranged lung cancer, we established patient-derived ALK-rearranged NSCLC cell line models from a treatment-naïve patient and from the same subsequently alectinib-refractory patient. We hypothesized that the establishment of the paired cell line model will clarify the mechanisms responsible for the development of alectinib resistance by comparing its properties, and will provide a new bioresource for future research on ALK-rearranged NSCLC. To the best of our knowledge, a patient-derived paired cell line model has not yet been successfully established to investigate ALK inhibitor resistance. We herein report that MET and Src played a key role in alectinib resistance as a dual salvage signaling pathway using the model.

Materials and Methods

Clinical information and procedures for obtaining informed consent

Clinical information was obtained from electronic medical records at the institution. The study protocol had been prepared in accordance with the Declaration of Helsinki. The patient provided written informed consent for this study. This study was approved by the Kyoto University Graduate School and Faculty of Medicine Ethics Committee (certification number: R0996).

Establishment of a clinical paired resistant model (CPRM)

The CPRM for alectinib consisted of 2 cell lines, KTOR1 and KTOR1-RE (*EML4-ALK* variant 1 E13; A20), which were established from a patient with ALK-rearranged NSCLC who regularly visited Kyoto University Hospital. The schematic explanation for this model was shown in Fig. 1A. Two-hundred milliliters of pleural effusion was obtained before first-line treatment with alectinib (KTOR1). When the disease progressed, pleural effusion was again collected (KTOR1-RE). Tumor cells were immediately separated from pleural effusion by centrifugation. Red blood cells were removed using Red Blood Cell Lysis Buffer by Roche Diagnostics (Basel, Switzerland). Tumor cells were cultured and maintained in alectinib-free RPMI 1640 medium (Nacalai Tesque, Kyoto, Japan) supplemented with 8% heat-inactivated FBS (Sigma-Aldrich, St. Louis, Missouri United States) and 1% Penicillin/Streptomycin (Gibco, Waltham, Massachusetts, USA) at 37.0°C in 5% CO_2.

Cell lines and reagents

The NCI-H2228 (*EML4-ALK* variant 3a/b E6; A20) cell line was purchased from the American Type Culture Collection in 2016. PC-9 cells (epidermal growth factor receptor: EGFR Ex19 del) were purchased from European Collection of Cell Cultures in 2014. The alectinib-resistant cell line, H2228-AR1S, was established by exposing NCI-H2228 cells to 300 nM of alectinib *in vitro* for 3 months. All experiments, including those using KTOR1 and KTOR1-RE cells, were performed with cells that were within 10 passages. All cells were tested in 2017 for Mycoplasma using the MycoAlert™ Mycoplasma Detection Kit (Lonza, Basel, Switzerland). Alectinib was kindly provided by Chugai Pharmaceutical Co., Ltd. Saracatinib and crizotinib were purchased from LC Laboratories (Woburn, MA, USA). PHA-665752 was purchased from Sigma-Aldrich. Alectinib, crizotinib, saracatinib, and PHA-665752 were dissolved in dimethyl sulfoxide (DMSO) (Nacalai Tesque) at a concentration of 5 mmol/L. DMSO was also used as a vehicle control.

Detection of the EML4-ALK rearrangement

Total RNA was extracted from the cell lines and purified using the PureLink® RNA Mini Kit (Ambion, Waltham, Massachusetts, USA). The expression of mRNA for the fusion protein *EML4-ALK* was examined using a reverse transcription polymerase chain reaction (RT-PCR). Previously described primers were used. (17) (Table S2) The PCR product was sequenced by Sanger's method using a 3130xl Genetic Analyzer (Applied Biosystems, Waltham, Massachusetts, USA). The protein expression of EML4-ALK was examined by immunoblotting.

Cell viability and drug sensitivity assays

Cells (5,000 cells/well) were cultured in 96-well plates overnight and incubated with stepwise concentrations of indicated drugs or vehicle control medium for 72 hours. Three independent experiments were performed. Viable cells were quantified using the CellTiter-Glo 2.0 Luminescent Cell Viability Assay (Promega, Fitchburg, Wisconsin, United States). Luminescence was measured by ARVO X3 (PerkinElmer, Waltham, MA, USA). Half maximal (50%) inhibitory concentration (IC_{50}) values were calculated using a non-linear regression model with a sigmoidal dose response by GraphPad Prism 7.0 (GraphPad software, La Jolla, CA, United States).

Cell growth assay

Cell growth assays were performed in accordance with previous reports. (18) Cells (5,000 cells/well) were cultured in 96-well plates. At 24 hours, all plates were brought to the indicated drug concentration or vehicle controls, and one plate representing the baseline plate was immediately frozen (-80°C). After incubations for 6-80 hours, remaining value plates were frozen (-80°C). After freezing, the value and baseline plates were thawed simultaneously, and viable cell numbers were quantified using CellTiter-Glo. The relative cell number was calculated with the formula: (Value-Baseline)/Baseline. Three independent experiments were performed. We had verified that one freezing and thawing procedure has little effect on CellTiter-Glo luminescence signals in our laboratory. (Fig. S1A)

Apoptosis assay

Cells (2,000 cells/well) were cultured in 386-well plates overnight and incubated with stepwise concentrations of drugs for 24 hours. Caspase 3/7 activities were tested using the Caspase-Glo 3/7 Assay (Promega) according to the manufacturer's recommendations. Three independent experiments were performed.

Immunoblotting

SDS-PAGE and immunoblotting were performed as described previously. (19) tALK, pALK (pY1604), tAkt, pAkt (pS473), tERK1/2, pERK1/2 (pT202/pY204), cMET, tSrc, pPaxillin (pY118), GAPDH, and secondary antibodies were purchased from Cell Signaling Technology (Danvers, Massachusetts, United States). The pMET (pY1234) antibody was purchased from GeneTex (Irvine, CA, United States). The vinculin antibody was purchased from Abcam (Cambridge, UK). The primary (1:1000) and secondary (1:2000) antibodies were diluted with 2.5% bovine serum albumin (BSA) / tris-buffered saline with tween 20 (TBS-T). BSA was purchased from Nacalai Tesque.

Phosphoproteome analysis

Cells were solubilized with lysis buffer (8 M urea and 4% (w/v) SDS in 50 mM Tris–HCl, pH 7.5) and incubated at 95°C for protein extraction. Cell lysates were sonicated on ice using the Bioruptor UCD-250T (Cosmo Bio, Tokyo, Japan). The solution was subjected to chloroform/methanol precipitation. (20) Proteins were reduced by dithiothreitol (10 mM) at 37°C for 30 min, and iodoacetamide (50 mM) was added. Sequencing-grade modified

trypsin (Promega, 2 μg) was added to the protein solution and incubated overnight. Peptide concentrations were measured using the BCA assay and adjusted to 10 μg/μL. Phosphopeptides were enriched using Titansphere Phos-TiO reagents (GL science, Osaka, Japan). The phosphopeptides obtained were labeled with a tandem mass tag (Thermo Fisher Scientific), as described by Aburaya et al. (21) Proteome analyses were performed using an LC-MS system (LC, UltiMate 3000 RSLCnano System, and MS, LTQ Velos Orbitrap mass spectrometer; Thermo Fisher Scientific) equipped with a long monolithic silica capillary column (490 cm in length, 0.075 mm ID; Kyoto Monotech, Kyoto, Japan). Combined spectrometric data were used for phosphopeptide identification and quantification. Phosphopeptides were identified using MASCOT (Matrix Science, London, UK) against UniProt (2002–2015 UniProt Consortium, EMBL-EBI) containing 20210 sequences, with a precursor mass tolerance of 20 ppm, fragment tolerance of 50 mmu, and strict specificity allowing for up to one missed cleavage. Data were then filtered at a q-value ≤ 0.01 corresponding to a 1% false discovery rate on a spectral level.

Quantitative reverse transcriptional polymerase chain reaction (qRT-PCR)

Total RNA was extracted from cultured cells using PureLink® RNA mini kit (Thermo Fisher Scientific). Gene expression was measured via a qRT-PCR assay with each reaction containing 100 ng of total RNA with One Step SYBR® PrimeScript™ RT-PCR Kit II (Takara-Bio, Shiga, Japan) and a primer pair designed to amplify target mRNA. (Table S3) Reactions were run on a 7300 Real Time PCR System (Applied Biosystems) for quantitation.

Transfection of small interfering RNA (siRNA)

siRNA oligonucleotides for *MET* and *SRC* were purchased from Thermo Fisher Scientific (Stealth RNAi^{TM} siRNA). Cells (5.0×10^5) were transfected with siRNA oligonucleotides with a final RNA concentration of 20 nM using Lipofectamine® RNAiMAX Transfection Reagent (Invitrogen, Waltham, Massachusetts, United States). A reverse transfection method was performed according to the manufacturer's instructions. After a 48-h incubation, medium was changed and transfected cells were exposed to the indicated concentrations of drugs. After 6 hours of drug exposure (54 hours after transfection), total protein was extracted for immunoblotting. In the cell viability assay, transfected cells were detached 24 hours after transfection, and cells (5000/well) were cultured in 96-well plates for 24 hours. Forty-eight hours after transfection, the indicated concentrations of drugs were applied to 96-well plates, which were then incubated for 72 hours. Cell viability was assessed as described above.

Xenograft models

Male or female SCID beige (CB17.Cg-*Prkdc*^{scid}*Lyst*$^{bg\text{-}J}$/CrlCrlj) mice were purchased at 6 weeks of age from Charles River Laboratories, Japan (Yokohama, Kanagawa, Japan). In order to generate the xenograft model, cells (1.5×10^6) were suspended in Matrigel® (Corning, NY, United States) and injected subcutaneously into the backs of mice. Twenty days after the tumor inoculation the treatment was started (day 0). Mice were randomized to receive vehicle, crizotinib (25 mg/kg/day), saracatinib (25 mg/kg/day), or a combination daily by oral gavage.

Tumor volumes were assessed using caliper measurements and calculated with the formula (Length × Width × Width) *0.51. All animal experiments and research plans were approved by the Animal Research Committee of Kyoto University (ID: MedKyo 17270) and were conducted in accordance with ARRIVE guidelines.

Statistics

Continuous variable data were expressed as the mean ± SEM. The significance of differences was assessed by the two-tailed unpaired Mann-Whitney U test. When the mean values of more than three groups were compared, P-values of all combinations were calculated using Tukey's multiple comparison test. P-values of <0.05 were defined as significant. All statistical analyses were performed using JMP Pro version 12.0 (SAS Institute, Inc., Cary, NC, United States) and visualized by GraphPad Prism 7.

Results

Establishment of the patient-derived ALK-rearranged paired resistant model

A CPRM for alectinib was established (Fig. 1A). A 29-year-old female was diagnosed with ALK-rearranged NSCLC in 2014 at Kyoto University Hospital. The *EML4-ALK* rearrangement was clinically diagnosed using fluorescent *in situ* hybridization. The patient was enrolled in a phase III clinical trial of alectinib (J-ALEX). (11) An evaluation performed 8 weeks after the initiation of alectinib revealed a strong response to the treatment; pleural effusion on the right side markedly decreased. Seven months later, disease progression, as indicated by increased pleural effusion on the left side, was observed (Fig. 1B). During the treatment, pleural effusion was collected twice: when the patient was treatment naive (KTOR1 cell, in 2014) and when the tumor was refractory to alectinib (KTOR1-RE cell, in 2015), and 2 cell lines were established (Fig. 1B). In the presence of 300 nmol/L (nM) of alectinib, the number of KTOR1 cells decreased, whereas KTOR1-RE cells grew slowly (Fig. 1C). Total RNA was extracted from the two cell lines and RT-PCR using *EML4-ALK* detection primers indicated mRNA for the EML4-ALK fusion protein in the KTOR1 and KTOR1-RE cells. Sequencing of the amplified PCR product revealed that the fusion type of *EML4-ALK* was variant 1 (Fig. 1D). Immunoblotting detected the expression and phosphorylation of EML4-ALK (EML4-pALK) fusion protein variant 1 in KTOR1 and KTOR1-RE cells (Fig. 1E). Exon sequencing using ALK exon sequencing primers (Table S1) indicated no secondary mutations in the coding region of ALK tyrosine kinase in KTOR1 or KTOR1-RE (Fig. 1F, Fig. S1B-G).

Stable resistance to ALK inhibitors in alectinib-resistant cells (KTOR1-RE)

The sensitivities of KTOR1 and KTOR1-RE to ALK inhibitors were examined. NCI-H2228 and PC-9 cells were also assessed simultaneously as responding and non-responding controls, respectively. KTOR1 cells were as sensitive to alectinib and crizotinib as H2228 cells. KTOR1-RE cells were resistant to alectinib, but seemed to be relatively sensitive to crizotinib (Fig. 2A, B, Fig. S2A, B). KTOR1 and KTOR1-RE cells were bulk cell lines without single cell cloning; therefore, they were potentially heterogeneous. In order to confirm the stability of the experiment, KTOR1 and KTOR1-RE were cultured for 6 months in alectinib-free medium and passaged 20 times. No significant difference was observed in alectinib sensitivity between the high and low passage cell lines

(Fig. S2C).

Alectinib resistance in KTOR1-RE was independent of ALK

In order to clarify whether the survival of KTOR1-RE cells depends on ALK signaling during the alectinib treatment, we assessed the phosphorylation of EML4-ALK and its downstream signaling molecules in the presence of stepwise concentrations of alectinib. EML4-pALK was inhibited in KTOR1 and KTOR1-RE by a low dose of alectinib (30 nM), whereas that of its downstream signaling molecules, Akt (pAkt) and ERK1/2 (pERK1/2), was only inhibited in KTOR1. pAkt and pERK1/2 are key molecules and activation markers for phosphatidylinositol-3 kinase (PI3K) /Akt pathway and mitogen activated protein kinase (MAPK) pathway, respectively, which maintains survival, cell proliferation, and anti-apoptosis. The downstream signaling molecules of KTOR1-RE were not inhibited in the presence of a high dose of alectinib (1,000 nM). This result suggested that as yet unidentified salvage signaling pathways maintained downstream signaling independent of EML4-ALK (Fig. 2C). Next, the phosphorylation of EML4-ALK and its downstream signaling molecules in the presence of crizotinib was evaluated. A high dose of crizotinib (300 nM-3,000 nM) inhibited EML4-pALK and pAkt both in KTOR1 and KTOR1-RE. pERK1/2 was also inhibited more by the high dose of crizotinib than in its absence, whereas phosphorylation was maintained slightly better than that with alectinib in KTOR1, which strongly inhibited pERK1/2 (Fig. 2D). MET phosphorylation (pMET) was greater in KTOR1-RE cells than in KTOR1 cells. As expected, crizotinib inhibited pMET, whereas alectinib did not (Fig. 2C, D). We focused on MET as a key molecule in the salvage pathway that maintained downstream signaling. The clinical course of the patient was partially consistent with the hypothesis that MET is involved in salvage signaling. Although the crizotinib treatment achieved stable disease in the patient after KTOR1-RE cells were derived, its PFS was limited to 15 weeks (Fig. 2E, F). The limited effects of crizotinib in the patient and in KTOR1-RE cells (Fig. 2A, B, E, F) suggested that another salvage pathway other than MET maintained cell proliferation and downstream signaling, MAPK pathway.

Activation of Src in KTOR1-RE

Phosphoproteomic approaches were performed to examine altered signaling pathways when KTOR1-RE cells were exposed to alectinib. We detected 1005 phosphorylated peptides (589 proteins) from the lysate of KTOR1 or KTOR1-RE cells, which included 35 phosphorylated tyrosines (Fig. 3A, Fig. S3A). Of the 35, three peptides (Paxillin, Protocadherin-1, and SSRP1) increased, particularly in KTOR1-RE cells, when cells were exposed to 0.3 μM of alectinib (Fig. 3B). Paxillin is a known substrate of the proto-oncogene tyrosine-protein kinase Src, and its phosphorylation is a marker for Src activity. Among the 1005 phosphorylated peptides (589 proteins), the phosphorylation status changed by more than 2-fold in 210 peptides (174 proteins) (Fig. 3A, S3A, Data File S1). Gene ontology (GO) analysis of the 174 proteins revealed enrichment of "cell-cell adherens junctions" (GO: 0005913, P value: 7.30×10^{-25}) as a cellular component, and enrichment of "cadherin binding involved in cell-cell adhesion" (GO: 0098641, P value: 4.80×10^{-24}) as a molecular mechanism, which are consistent with Src activation (Fig. 3C, S3B, S3C). qRT-PCR suggested increased gene expression of *SRC* among Src kinase family

genes (Fig. 3D). Immunoblotting indicated that the protein expression of Src and phosphorylation of Paxillin (pPaxillin, Y118) increased in KTOR1-RE cells as well as pMET (Fig. 3E). Then, combination drugs that enhanced crizotinib sensitivity were examined. KTOR1-RE cells restored crizotinib sensitivity in combination with saracatinib, a selective Src family kinase inhibitor (IC_{50} of crizotinib: 9.4 μM with vehicle, and 1.2 μM in combination with 3 μM of saracatinib, relative ratio (RR): 7.83) (Fig. 3F).

Combination of saracatinib and MET inhibitors overcame alectinib resistance

The inhibition of Src and/or MET in KTOR1-RE cells using saracatinib and PHA-665752, a specific MET inhibitor, was evaluated. No significant differences were observed in sensitivity to saracatinib or PHA-665752 monotherapy among KTOR1, KTOR1-RE, and H2228 cells. (Fig. 4A). We then examined the effects of combination therapy with a fixed dose of saracatinib and PHA-665752. The exposure dose of saracatinib was selected as 3 μM, since the cell viability of KTOR1-RE was not altered in the presence of 3 μM of saracatinib, but incubation with 10 μM of the agent significantly reduced cell number (Fig. 4A). The 3 μM of saracatinib was sufficient to inhibit phosphorylation of Paxillin (Fig. S4A). In the same manner, the exposure dose of PHA-665752 was selected as 3 μM (Fig. 4A). The cell number of KTOR1-RE increased during monotherapy with alectinib, PHA-665752, or saracatinib, but decreased during triple therapy with the three agents (Fig. 4B, C). An apoptosis assay using Caspase-glo indicated that caspase 3/7 activity was significantly (3.56-fold) increased in KTOR1-RE cells treated with the triple therapy (Fig. 4B, D). Exposure to both alectinib and PHA-665752 downregulated pAkt in KTOR1-RE, but pERK1/2 was inhibited only when cells were exposed to three inhibitors (Fig. 4B, E). A drug sensitivity assay indicated that KTOR1-RE cells partially restored alectinib sensitivity in the presence of saracatinib, and greatly (17.2-fold in IC_{50}) restored sensitivity in combination with saracatinib plus PHA-665752 (Fig. 4B, F). The first generation ALK inhibitor crizotinib is clinically available and the compound also inhibits MET. In KTOR1-RE, exposure to high dose crizotinib (1 μM) inhibited pMET, EML4-pALK, and pAkt, but pERK1/2 signaling was maintained and cell number was increased compared with baseline (Fig. 2D, Fig. S4C, E). Combination therapy of high dose crizotinib and 3 μM of saracatinib induced inhibition of both pAkt and pERK1/2, decreased cell number, and increased caspase 3/7 activity (Fig. S4B-E). In order to evaluate the therapeutic significance of salvage signaling caused by MET and Src, a xenograft tumor mouse model of KTOR1-RE was evaluated. Xenograft mice were treated with vehicle, crizotinib monotherapy, saracatinib monotherapy, or combination therapy. Vehicle, saracatinib monotherapy, and crizotinib monotherapy did not inhibit tumor growth, whereas combination therapy with crizotinib and saracatinib blocked the growth of KTOR1-RE xenograft tumors (Fig. 4G).

Inhibition of salvaged downstream signaling was specific for Src and MET activity

In order to clarify whether the inhibition of growth and downstream signaling was specific to Src and MET activities, *SRC* and *MET* gene knockdown using siRNA was evaluated. The knockdown of *SRC* or *MET* did not suppress EML4-pALK, pAkt, and pERK1/2 (Fig. 5A, B). Knockdown of *MET* in the presence of alectinib inhibited pAkt, but did not inhibit pERK1/2. The combined knockdown of *MET* and *SRC* in the presence of

alectinib suppressed both pAkt and pERK1/2 (Fig. 5C, Fig. S5A), reduced cell number of KTOR1-RE (Fig. 5D, E, S5B), and increased caspase 3/7 activity as compared with alectinib monotherapy (1.69-fold in siMETSRC-A and 1.90-fold in siMETSRC-B) (Fig. 5D, F, Fig. S5C). The knockdown of *SRC* in the presence of crizotinib also suppressed downstream signaling (Fig. S5D), reduced cell number (Fig. 5E, S5E), and increased caspase 3/7 activity. (Fig. 5F, Fig. S5F).

Cells with high MET and/or Src activity were present under treatment-naïve conditions (KTOR1)

To obtain evidence to support cells with high MET and/or Src activity initially being present, the single cell cloning of KTOR1 using limited dilution was performed. We seeded KTOR1 at the concentration of 0.3-1.0 cells/well to three 96-well plates (288 wells) for three times (total 864 wells), but only 3 clones (KTOR1-A, B, C) were obtained, that might suggest the majority of KTOR1 cells could not survive in a single cell environment. The 3 cloned strains had high MET and/or Src activity and less sensitivity to alectinib than KTOR1 parental cells (Fig. 6A, B). Next, in order to evaluate whether Src and MET are associated with the initial survival of KTOR1 cells, we explored signal alterations when exposing KTOR1 to 300 nM of alectinib or vehicle for several days. Although the activity of EML4-ALK in KTOR1 was suppressed after 4 or 8 days of alectinib exposure, pAkt was maintained, and the phosphorylation of ERK1/2 and Paxillin was increased (Fig. S6A).

Activation of MET and Src in another alectinib-exposed ALK-rearranged cell line

To confirm the generality, an alectinib-resistant ALK-rearranged NSCLC cell line (H2228-AR1S) was established from NCI-H2228 cells. (Fig. 6C) The H2228-AR1S cell line grew in the presence of 1 μM of alectinib, 3 μM of crizotinib, 3 μM of saracatinib, or 3 μM of PHA-665752. Triple therapy with alectinib, saracatinib, and PHA-665752 or combination therapy with crizotinib and saracatinib reduced the number of H2228-AR1S cells (Fig. 6D, E), increased caspase 3/7 activity (Fig. 6D, F), and inhibited both MAPK and PI3K/Akt signaling (Fig. 6D, G, S6B). Immunoblotting of the 4 sub-clones of H2228-ARIS cells suggested that the H2228-AR1S cell line had heterogeneity, containing subpopulations with high MET and/or Src activity (Fig. 6H). These results demonstrated that inhibition of MET was sufficient to inhibit pAkt in the presence of alectinib, but did not downregulate MAPK pathway, pERK1/2, and that MET, Src, and ALK maintained MAPK pathway (Fig. 7). The inhibition of both Src and MET was needed to sensitize cells to ALK inhibitors.

Discussion

We herein provided a CPRM with an ALK rearrangement from a patient with NSCLC. We consider the KTOR1 and KTOR1-RE cell lines to be new bioresources that may be cultured, passaged, and applied to investigations on ALK-positive lung cancer. Using this CPRM for alectinib, we demonstrated that two salvage signaling pathways, Src and MET, were involved in drug resistance, anti-apoptosis, and tumor growth. Triple inhibition of Src, ALK, and MET effectively overcame drug resistance. To the best of our knowledge, drug-resistant mechanisms have not yet been investigated using CPRM.

The present study suggested potential advantages of CPRM that will advance research on drug resistance. Data

obtained from clinical samples reflect events in the patient, but evaluation of a few clinical samples may be ambiguous because clinical patients have intra- and inter-tumor heterogeneity. (22,23) Using CPRM, however, comparisons of patient-derived resistant cells with patient-derived treatment-naïve cells reduce noise and provide clear information on properties acquired during treatments. For example, a phosphoproteome analysis indicated numerous phosphorylated proteins in KTOR1-RE cells treated with alectinib, whereas most phosphopeptides/phosphoproteins were excluded because these were phosphorylated to a similar extent in KTOR1 cells treated with alectinib. We may not have been unable to focus on the phosphorylation of Paxillin if treatment-naïve KTOR1 cells had not been available. This approach permits drug-resistant mechanisms to be elucidated while investigating relatively fewer patients, without exploring the common characteristics of numerous drug-resistant patients, and may be suitable for research on rare cancers.

Extensive efforts are needed to refine and continuously establish CPRM. Patients need to be followed up in one institution from biopsy to diagnosis, treatment, and the acquisition of resistance. Furthermore, efforts should be made to establish cell lines for all potential patients, because biopsy is usually performed before definite diagnosis. Additionally, the success rate of cell line establishment from pleural effusion is approximately 50%, and lower from biopsy samples. (18) We established 5 treatment-naïve cultivable cell lines from NSCLC and are now following patient treatment courses.

This is the first study to show that dual salvage signaling from Src and MET is associated with the development of alectinib resistance. (Fig. 7) Src is a non-receptor tyrosine kinase, the activity of which correlates with a poor prognosis and advanced malignancy in a number of human cancers. (24) The Src/Paxillin pathway plays an important role in anchorage-independent growth and, in our results, phosphoproteome analysis detected significant enrichment in phosphoproteins related to cell adhesion when KTOR1-RE was incubated with alectinib (Fig.3C). Anchorage-independent growth is potentially involved in determining response. In addition, we isolated only 3 single cell clones from KTOR1 cells, which supports majority of KTOR1 cells could not survive in the single cell environment. Considering that days of alectinib exposure induced increased phosphorylation of Paxillin in KTOR1 (Fig. S6B), Src/Paxillin signals also could be associated with initial response to alectinib exposure.

Src is also a key molecule conferring resistance to crizotinib in ALK-rearranged lung cancer. Crystal et al. demonstrated that the inhibition of Src using saracatinib enhanced crizotinib sensitivity in 7 out of 12 crizotinib-resistant cell lines. (18) In second generation ALK inhibitors, only *in vitro* studies suggested that saracatinib sensitized ceritinib-resistant ALK-rearranged lung cancer. (25) Various Src inhibitors have been developed including dasatinib, bosutinib, and saracatinib, and their safety profiles have been confirmed. (26-28) Our result provided a rationale to conduct future clinical trials on Src inhibitors in combination with ALK inhibitors in patients with no secondary mutations.

MET bypass signaling as a cause of ALK-TKI resistance has not yet been reported in detail because crizotinib, which also inhibits MET signaling, has taken a leading role in the treatment of ALK-rearranged NSCLC. A previous study showed that MET alternative signaling was not associated with ALK-TKI resistance in 12 ALK-TKI-resistant cell lines. (18) Our results were not contradictory to these findings because the resistant cell lines in that study had been established by exposing ALK-rearranged cell lines to crizotinib or were derived from patients who had received crizotinib. There is a supportive evidence that HGF/cMET signaling pathway potentially salvages downstream signaling and combination inhibition of HGF/cMET and ALK limitedly inhibit downstream signaling, but the generality has not been confirmed because the report demonstrated bypass signaling from MET in one alectinib-resistant cell line established *in vitro*. (14,29) In a case report, crizotinib was effective after the development of alectinib resistance in a patient with a *MET* gene amplification. (30) Our results added a novel evidence that MET bypass signaling was associated with alectinib resistance in the clinical settings . The importance of MET bypass signaling may be going to increase since inhibitors with high affinity and specificity to ALK may replace crizotinib as the favored first-line therapy and the mechanisms of ALK inhibitor resistance may also change. (10-12) The identification of gatekeeper mutations and the development of more specific inhibitors, such as third generation ALK inhibitors brigatinib and lorlatinib (31-33), are important, but resistance due to salvage signaling also needs to be overcome.

In the development of novel targeted therapy for salvage signaling, the potential of two or more bypass salvage pathways complicates appropriate combinations of inhibitors. For example, research on targeted therapy for salvage signaling is more advanced in EGFR-TKI, (15) whereas clinical trials targeting MET, the most common salvage signal, were negative. (34) Since multiple salvage signaling pathways have been implicated and clinical surrogate markers have not yet been identified, difficulties are associated with establishing appropriate combination treatments for EGFR-positive NSCLC. This is also the case for ALK-TKIs. Preclinical and clinical studies showed that EGFR, HER2, KIT, KRAS, and IGF were associated with ALK inhibitor resistance as alternative salvage signaling pathways, (8,14,35) which indicates numerous potential combination therapies. Biomarkers to screen and individualize various bypass signaling pathways are needed. Drug arrays and shRNA libraries are potential solutions to these issues. (18,36)

This study has 3 major limitations. First, saracatinib is a multiple kinase inhibitor that also inhibits various tyrosine kinases. However, our in vitro experiment using siRNA supported that the resistance mechanism in KTOR1-RE was specific for Src and MET. Second limitation is that we presented only one CPRM. Then, we identified co-activation of MET and Src in conventional alectinib-resistant model H2228-AR1S, and combination inhibition of Src and MET restored alectinib sensitivity. Dual salvage signaling from MET and Src could be generated from monoclonal cultured cells by exposing these cells to alectinib, that supports generality of our findings. Finally, we examined the efficacy of the combination therapy of crizotinib and saracatinib *in vivo* and did not evaluate the triple therapy with alectinib, PHA-665752, and saracatinib. To identify specific resistance mechanisms with alectinib, it may be necessary to evaluate the effect on xenografts with the triple

therapy. From a clinical point of view, however, preclinical evidence on crizotinib-based therapy for alectinib-resistant models would be worthy of literature. This is because crizotinib is the most evident MET inhibitor of safety and efficacy in human, and a phase II clinical trial evaluating crizotinib monotherapy after acquiring alectinib-resistance is ongoing. (14) On the other hand, PHA-665752 has no phase I trials to evaluate the safety and efficacy for humans.

In summary, the present results indicated that dual salvage bypasses were associated with the development of alectinib resistance in a patient with ALK-rearranged NSCLC, and suggested the importance of establishing patient-derived paired cell lines, before treatment and after the development of resistance, for research on drug resistance. These results will contribute to the development of new therapeutic and research strategies for patients with ALK-rearranged NSCLC.

Acknowledgments

We are grateful to Yoshie Koyama and Yuko Maeda, the Department of Respiratory Medicine, Graduate School of Medicine, Kyoto University for their assistance in performing experiments.

Author contributions

T.T. designed the experiments, performed cell line, *in vitro*, and *in vivo* studies, and wrote the manuscript. H.O. identified the patient, designed and supervised the experiments, and wrote the manuscript. T.N., T.F., Y.Yasuda, and Y.Yagi performed cell line and *in vitro* studies. H.A., R.O., K.U., and K.H. performed repeat biopsies and provided study material. W.A., S.A., and M.U. designed, performed, analyzed the results, and wrote the manuscript of the phosphoproteome analysis. K.F. and Y.Yoshimura supervised *in vitro* and *in vivo* assays and appropriate drug usage. T.H. and Y.K supervised experiments. All authors revised and approved the article for important intellectual content.

References

1. Paez JG, Janne PA, Lee JC, Tracy S, Greulich H, Gabriel S*, et al.* EGFR mutations in lung cancer: correlation with clinical response to gefitinib therapy. *Science* **2004**;304:1497-500
2. Maemondo M, Inoue A, Kobayashi K, Sugawara S, Oizumi S, Isobe H*, et al.* Gefitinib or chemotherapy for non-small-cell lung cancer with mutated EGFR. *N Engl J Med* **2010**;362:2380-8
3. Soda M, Choi YL, Enomoto M, Takada S, Yamashita Y, Ishikawa S*, et al.* Identification of the transforming EML4-ALK fusion gene in non-small-cell lung cancer. *Nature* **2007**;448:561-6
4. Kwak EL, Bang YJ, Camidge DR, Shaw AT, Solomon B, Maki RG*, et al.* Anaplastic Lymphoma Kinase Inhibition in Non-Small-Cell Lung Cancer. *N Engl J Med* **2010**;363:1693-703
5. Solomon BJ, Mok T, Kim DW, Wu YL, Nakagawa K, Mekhail T*, et al.* First-line crizotinib versus chemotherapy in ALK-positive lung cancer. *N Engl J Med* **2014**;371:2167-77
6. Doebele RC, Pilling AB, Aisner DL, Kutateladze TG, Le AT, Weickhardt AJ*, et al.* Mechanisms of

resistance to crizotinib in patients with ALK gene rearranged non-small cell lung cancer. *Clin Cancer Res* **2012**;18:1472-82

7. Choi YL, Soda M, Yamashita Y, Ueno T, Takashima J, Nakajima T*, et al.* EML4-ALK mutations in lung cancer that confer resistance to ALK inhibitors. *N Engl J Med* **2010**;363:1734-9
8. Katayama R, Shaw AT, Khan TM, Mino-Kenudson M, Solomon BJ, Halmos B*, et al.* Mechanisms of acquired crizotinib resistance in ALK-rearranged lung Cancers. *Sci Transl Med* **2012**;4:120ra17
9. Sasaki T, Koivunen J, Ogino A, Yanagita M, Nikiforow S, Zheng W*, et al.* A novel ALK secondary mutation and EGFR signaling cause resistance to ALK kinase inhibitors. *Cancer Res* **2011**;71:6051-60
10. Sakamoto H, Tsukaguchi T, Hiroshima S, Kodama T, Kobayashi T, Fukami TA*, et al.* CH5424802, a selective ALK inhibitor capable of blocking the resistant gatekeeper mutant. *Cancer Cell* **2011**;19:679-90
11. Peters S, Camidge DR, Shaw AT, Gadgeel S, Ahn JS, Kim DW*, et al.* Alectinib versus Crizotinib in Untreated ALK-Positive Non-Small-Cell Lung Cancer. *N Engl J Med* **2017**;377:829-38
12. Hida T, Nokihara H, Kondo M, Kim YH, Azuma K, Seto T*, et al.* Alectinib versus crizotinib in patients with ALK-positive non-small-cell lung cancer (J-ALEX): an open-label, randomised phase 3 trial. *Lancet* **2017**;390:29-39
13. Seto T, Kiura K, Nishio M, Nakagawa K, Maemondo M, Inoue A*, et al.* CH5424802 (RO5424802) for patients with ALK-rearranged advanced non-small-cell lung cancer (AF-001JP study): a single-arm, open-label, phase 1-2 study. *Lancet Oncol* **2013**;14:590-8
14. Isozaki H, Ichihara E, Takigawa N, Ohashi K, Ochi N, Yasugi M*, et al.* Non-Small Cell Lung Cancer Cells Acquire Resistance to the ALK Inhibitor Alectinib by Activating Alternative Receptor Tyrosine Kinases. *Cancer Res* **2016**;76:1506-16
15. Yano S, Wang W, Li Q, Matsumoto K, Sakurama H, Nakamura T*, et al.* Hepatocyte growth factor induces gefitinib resistance of lung adenocarcinoma with epidermal growth factor receptor-activating mutations. *Cancer Res* **2008**;68:9479-87
16. Koivunen JP, Mermel C, Zejnullahu K, Murphy C, Lifshits E, Holmes AJ*, et al.* EML4-ALK fusion gene and efficacy of an ALK kinase inhibitor in lung cancer. *Clin Cancer Res* **2008**;14:4275-83
17. Soda M, Isobe K, Inoue A, Maemondo M, Oizumi S, Fujita Y*, et al.* A prospective PCR-based screening for the EML4-ALK oncogene in non-small cell lung cancer. *Clin Cancer Res* **2012**;18:5682-9
18. Crystal AS, Shaw AT, Sequist LV, Friboulet L, Niederst MJ, Lockerman EL*, et al.* Patient-derived models of acquired resistance can identify effective drug combinations for cancer. *Science* **2014**;346:1480-6
19. Ozasa H, Oguri T, Maeno K, Takakuwa O, Kunii E, Yagi Y*, et al.* Significance of c-MET overexpression in cytotoxic anticancer drug-resistant small-cell lung cancer cells. *Cancer Sci* **2014**;105:1032-9
20. Wessel D, Flugge UI. A method for the quantitative recovery of protein in dilute solution in the presence of detergents and lipids. *Anal Biochem* **1984**;138:141-3
21. Aburaya S, Esaka K, Morisaka H, Kuroda K, Ueda M. Elucidation of the recognition mechanisms for hemicellulose and pectin in Clostridium cellulovorans using intracellular quantitative proteome analysis. *AMB Express* **2015**;5:29

22. Shaw AT, Friboulet L, Leshchiner I, Gainor JF, Bergqvist S, Brooun A*, et al.* Resensitization to Crizotinib by the Lorlatinib ALK Resistance Mutation L1198F. *N Engl J Med* **2016**;374:54-61
23. Zhang J, Fujimoto J, Zhang J, Wedge DC, Song X, Zhang J*, et al.* Intratumor heterogeneity in localized lung adenocarcinomas delineated by multiregion sequencing. *Science* **2014**;346:256-9
24. Wheeler DL, Iida M, Dunn EF. The role of Src in solid tumors. *Oncologist* **2009**;14:667-78
25. Zhao Y, Yang Y, Xu Y, Lu S, Jian H. AZD0530 sensitizes drug-resistant ALK-positive lung cancer cells by inhibiting SRC signaling. *FEBS Open Bio* **2017**;7:472-6
26. McNeish IA, Ledermann JA, Webber L, James L, Kaye SB, Hall M*, et al.* A randomised, placebo-controlled trial of weekly paclitaxel and saracatinib (AZD0530) in platinum-resistant ovarian, fallopian tube or primary peritoneal cancerdagger. *Ann Oncol* **2014**;25:1988-95
27. Kaye S, Aamdal S, Jones R, Freyer G, Pujade-Lauraine E, de Vries EG*, et al.* Phase I study of saracatinib (AZD0530) in combination with paclitaxel and/or carboplatin in patients with solid tumours. *Br J Cancer* **2012**;106:1728-34
28. Baselga J, Cervantes A, Martinelli E, Chirivella I, Hoekman K, Hurwitz HI*, et al.* Phase I safety, pharmacokinetics, and inhibition of SRC activity study of saracatinib in patients with solid tumors. *Clin Cancer Res* **2010**;16:4876-83
29. Kogita A, Togashi Y, Hayashi H, Banno E, Terashima M, De Velasco MA*, et al.* Activated MET acts as a salvage signal after treatment with alectinib, a selective ALK inhibitor, in ALK-positive non-small cell lung cancer. *Int J Oncol* **2015**;46:1025-30
30. Gouji T, Takashi S, Mitsuhiro T, Yukito I. Crizotinib can overcome acquired resistance to CH5424802: is amplification of the MET gene a key factor? *J Thorac Oncol* **2014**;9:e27-8
31. Katayama R, Khan TM, Benes C, Lifshits E, Ebi H, Rivera VM*, et al.* Therapeutic strategies to overcome crizotinib resistance in non-small cell lung cancers harboring the fusion oncogene EML4-ALK. *Proc Natl Acad Sci U S A* **2011**;108:7535-40
32. Johnson TW, Richardson PF, Bailey S, Brooun A, Burke BJ, Collins MR*, et al.* Discovery of (10R)-7-amino-12-fluoro-2,10,16-trimethyl-15-oxo-10,15,16,17-tetrahydro-2H-8,4-(m etheno)pyrazolo[4,3-h][2,5,11]-benzoxadiazacyclotetradecine-3-carbonitrile (PF-06463922), a macrocyclic inhibitor of anaplastic lymphoma kinase (ALK) and c-ros oncogene 1 (ROS1) with preclinical brain exposure and broad-spectrum potency against ALK-resistant mutations. *J Med Chem* **2014**;57:4720-44
33. Zou HY, Friboulet L, Kodack DP, Engstrom LD, Li Q, West M*, et al.* PF-06463922, an ALK/ROS1 Inhibitor, Overcomes Resistance to First and Second Generation ALK Inhibitors in Preclinical Models. *Cancer Cell* **2015**;28:70-81
34. Spigel. DR, Edelman. MJ, O'Byrne. K, Paz-Ares. L, Shames. DS, Yu. W*, et al.* Onartuzumab plus erlotinib versus erlotinib in previously treated stage IIIb or IV NSCLC: Results from the pivotal phase III randomized, multicenter, placebo-controlled METLung (OAM4971g) global trial. *J Clin Oncol* **2014**;(suppl; abstr 8000); 32: 5s.
35. Tanizaki J, Okamoto I, Okabe T, Sakai K, Tanaka K, Hayashi H*, et al.* Activation of HER family signaling

as a mechanism of acquired resistance to ALK inhibitors in EML4-ALK-positive non-small cell lung cancer. *Clin Cancer Res* **2012**;18:6219-26

36. Manchado E, Weissmueller S, Morris JPt, Chen CC, Wullenkord R, Lujambio A*, et al.* A combinatorial strategy for treating KRAS-mutant lung cancer. *Nature* **2016**;534:647-51

Figure legends:

Figure 1

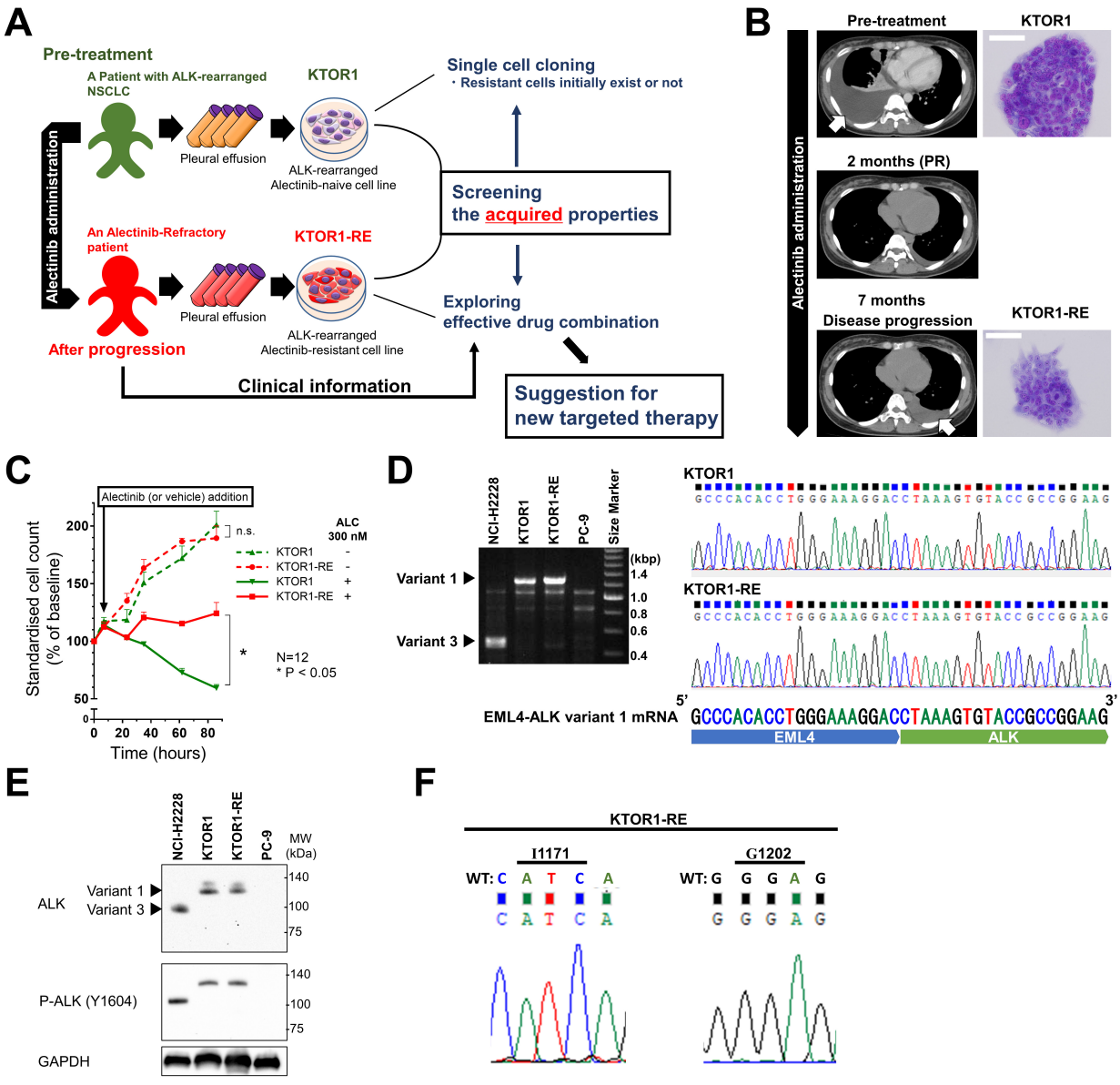

Fig. 1. Establishment of a patient-derived paired resistant model from a patient with ALK-rearranged NSCLC

(**A**) Schematic explanation of the clinical paired resistant model (CPRM). Tumor cells were obtained twice: pre-treatment and at disease progression. Properties acquired during the treatment were screened by comparing the two cell lines. The acquired properties were evaluated as therapeutic targets using resistant cells. (**B**) CT images in the clinical course of the patient (left side), and optical micrographs of cells stained using the Papanicolaou stain (right side). KTOR1 cells were established from pleural effusion collected from the right side before the treatment (white arrow) (top). The patient responded to alectinib (middle). KTOR1-RE cells were established from pleural effusion collected from the left side (white arrow) when disease progression was observed (bottom). Calibration bar = 200 micrometers. (**C**) Cell proliferation assay of KTOR1 and KTOR1-RE. Both cell lines were

incubated in medium with vehicle or 300 nM of alectinib. (**D**) Detection of mRNA for the EML4-ALK fusion protein. The PCR product specific for EML4-ALK was positive in NCI-H2228, KTOR1, and KTOR1-RE. PC-9 (adenocarcinoma, EGFR exon 19 del) is a negative control. (left) Sequencing using Sanger's method indicated EML4-ALK rearrangement variant 1 in KTOR1 and KTOR1-RE (right). (**E**) The protein expression and phosphorylation of the EML4-ALK fusion protein in NCI-H2228, KTOR1, and KTOR1RE indicated by immunoblotting. (**F**) Direct sequencing of the tyrosine kinase coding region in ALK. I1171 and G1202 are known mutations that confer alectinib resistance. KTOR1-RE cells did not have known resistant mutations.

Figure 2

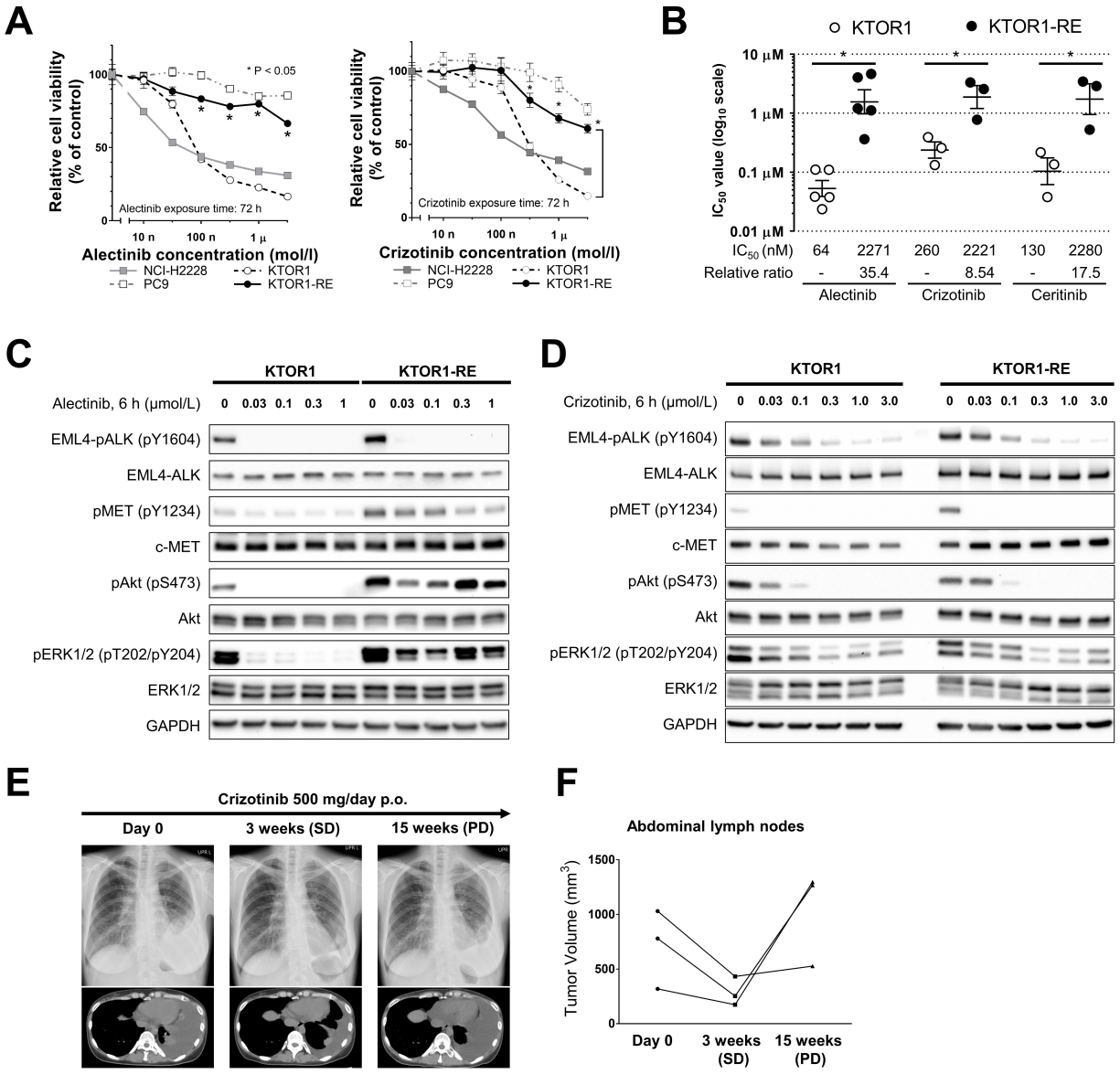

Fig. 2. Alectinib-refractory patient-derived cells were resistant to alectinib, whereas crizotinib was only partially effective.

(A) Cell viability assay on KTOR, KTOR1-RE, NCI-H2228, and PC9 cells in the presence of alectinib (left) or crizotinib (right). (B) IC_{50} values of cell lines treated with crizotinib, alectinib, and ceritinib. Data shown in the figure were obtained simultaneously. (C, D) KTOR1 and KTOR1-RE cells were treated with the indicated concentrations of alectinib (C) or crizotinib (D) for 6 h. Cell lysates were analyzed by immunoblotting with the indicated antibodies. (E, F) Clinical course of the patient during the crizotinib treatment after the tumor had acquired resistance to alectinib. (E) Crizotinib achieved stable disease by the 3-week evaluation and pleural effusion decreased. However, pleural effusion on the left side increased by 3 months. (F) Changes in abdominal lymph nodes also suggested that although crizotinib after alectinib was effective at 3 weeks, the effect was limited; size increased at 15 weeks.

Figure 3

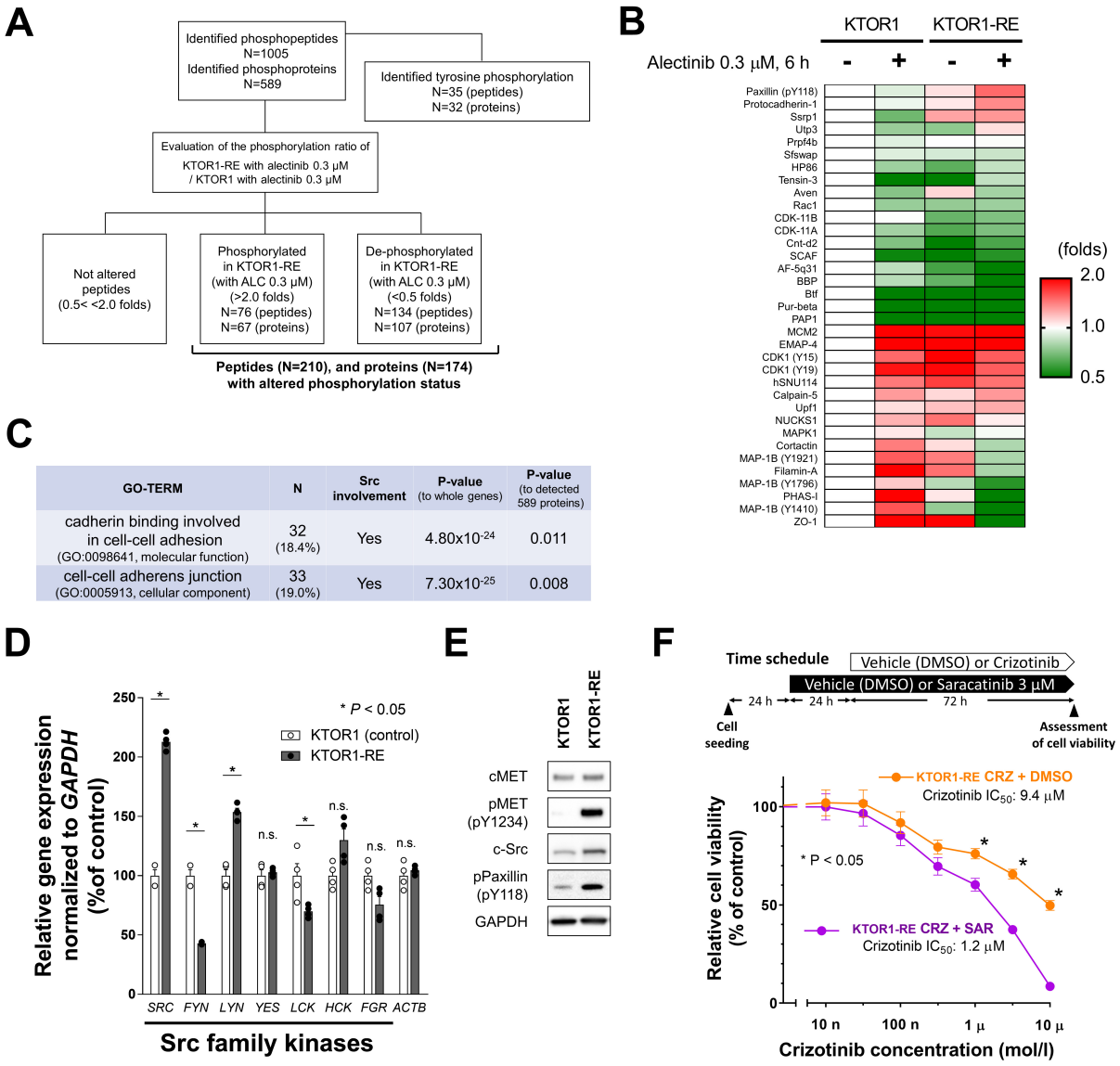

GO-TERM	N	Src involvement	P-value (to whole genes)	P-value (to detected 589 proteins)
cadherin binding involved in cell-cell adhesion (GO:0098641, molecular function)	32 (18.4%)	Yes	4.80×10^{-24}	0.011
cell-cell adherens junction (GO:0005913, cellular component)	33 (19.0%)	Yes	7.30×10^{-25}	0.008

Fig. 3. Src was another potential bypass salvage signal in KTOR1-RE cells.

(**A**) Summary of phosphopeptides and phosphoproteins identified by the phosphoproteome analysis. (**B**) Fold changes in tyrosine phosphorylation (Log2) in cells treated with 0.3 μM of the ALK inhibitor for 6 hours. (**C**) Gene ontology (GO) analysis of 174 proteins with an altered phosphorylation status. P-values were calculated using Fisher's test. (**D**) Evaluation of expressions of Src family kinase genes using quantitative reverse transcriptional PCR. The significance of differences between KTOR1 and KTOR1-RE was assessed by Mann-Whitney test in each gene expression. (**E**) Evaluation of MET phosphorylation, Src expression, and Paxillin phosphorylation. Cell lysates of KTOR1 and KTOR1-RE were analyzed using an immunoblotting assay with the indicated antibody. (**F**) Viability of KTOR1-RE cells treated with saracatinib or vehicle for 24 hours and then with the indicated concentrations of crizotinib for 72 h. Cell viability or number was quantified using the CellTiter-Glo assay. IC_{50} values are indicated in the figure.

Figure 4

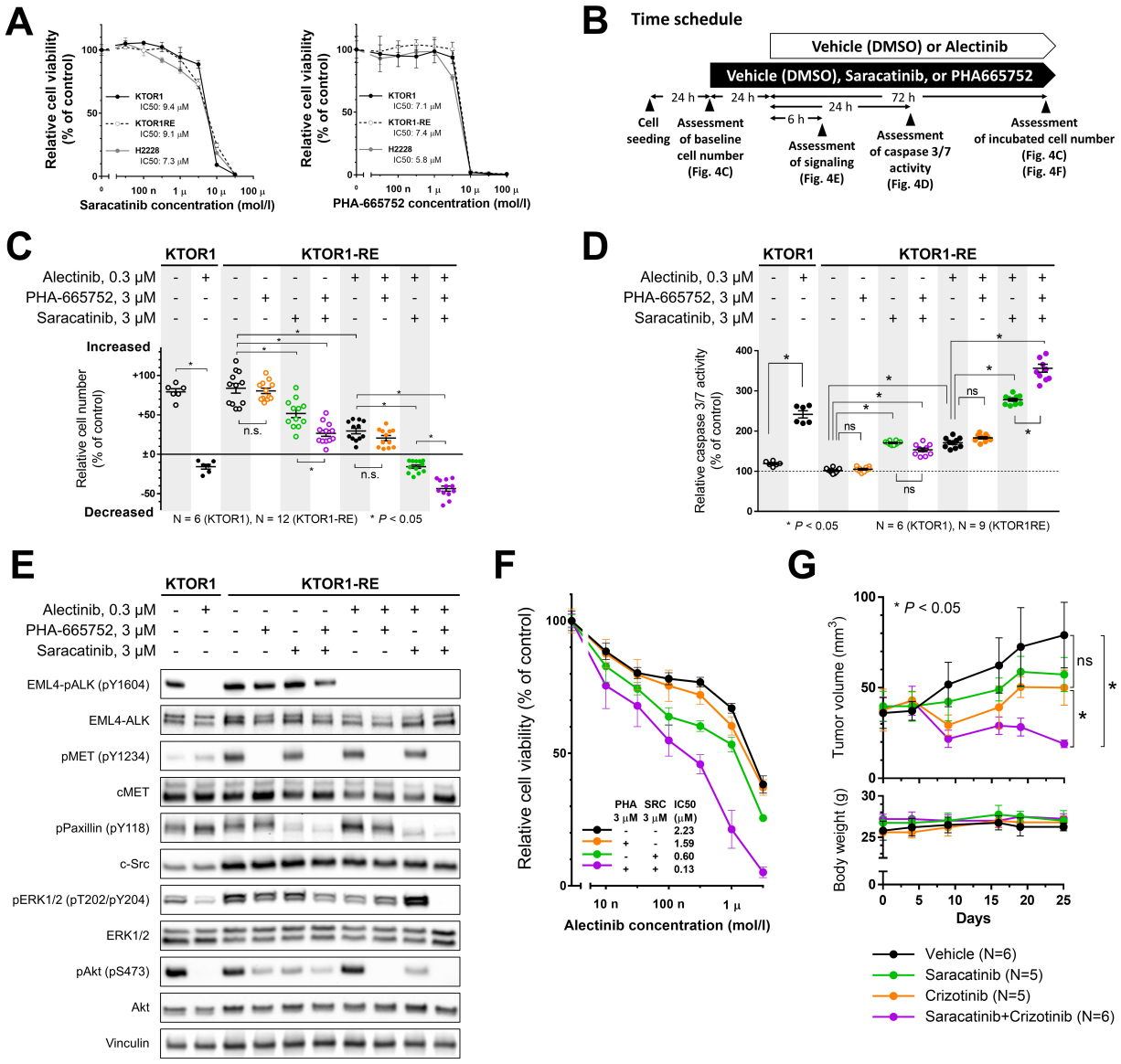

Fig. 4. Combination of saracatinib and MET inhibitors overcame alectinib resistance in KTOR1-RE cells. Cell viability or number was quantified using the CellTiter-Glo assay. IC_{50} values are shown in the figure. (**A**) Cell viabilities of the ALK-rearranged cell lines, H2228, KTOR1, and KTOR1-RE treated with stepwise concentrations of saracatinib (left) or PHA-665752 (right) for 72 h. (**B-E**) Cell growth, apoptosis, and signaling assays for KTOR1 and KTOR1-RE treated with alectinib, saracatinib, and/or PHA-665752. KTOR1 and KTOR1-RE cells were incubated with vehicle, PHA-665752, saracatinib, or a combination for 24 h, as indicated in the figure, and subsequently treated with alectinib. The assay time schedule was presented in (**B**). (**C**) A cell growth assay of KTOR1 and KTOR1-RE when cells were exposed to indicated agents. All columns were compared and P-value was calculated using Tukey test. (**D**) Caspase 3/7 activity was quantified using Caspase-Glo after a 24-h treatment with alectinib or vehicle. P-value was calculated using Tukey test.(**E**) A cell lysate was obtained after exposure to indicated drugs and analyzed by immunoblotting using the indicated antibody.

(**F**) A cell viability assay of KTOR1-RE cells treated with vehicle, PHA-665752, saracatinib, or a combination for 24 h, and then treated with alectinib for 72 h. (**G**) Effects of combination therapy with saracatinib and crizotinib on tumor growth and body weight in KTOR1-RE xenograft models. KTOR1-RE xenograft tumors were treated with vehicle, 25 mg/kg/day saracatinib, 25 mg/kg/day crizotinib, or a combination. Tumor sizes were statistically analyzed by Mann-Whitney test on day 25. Tumor volume (top) and body weight (bottom) curves. * $P < 0.05$.

Figure 5

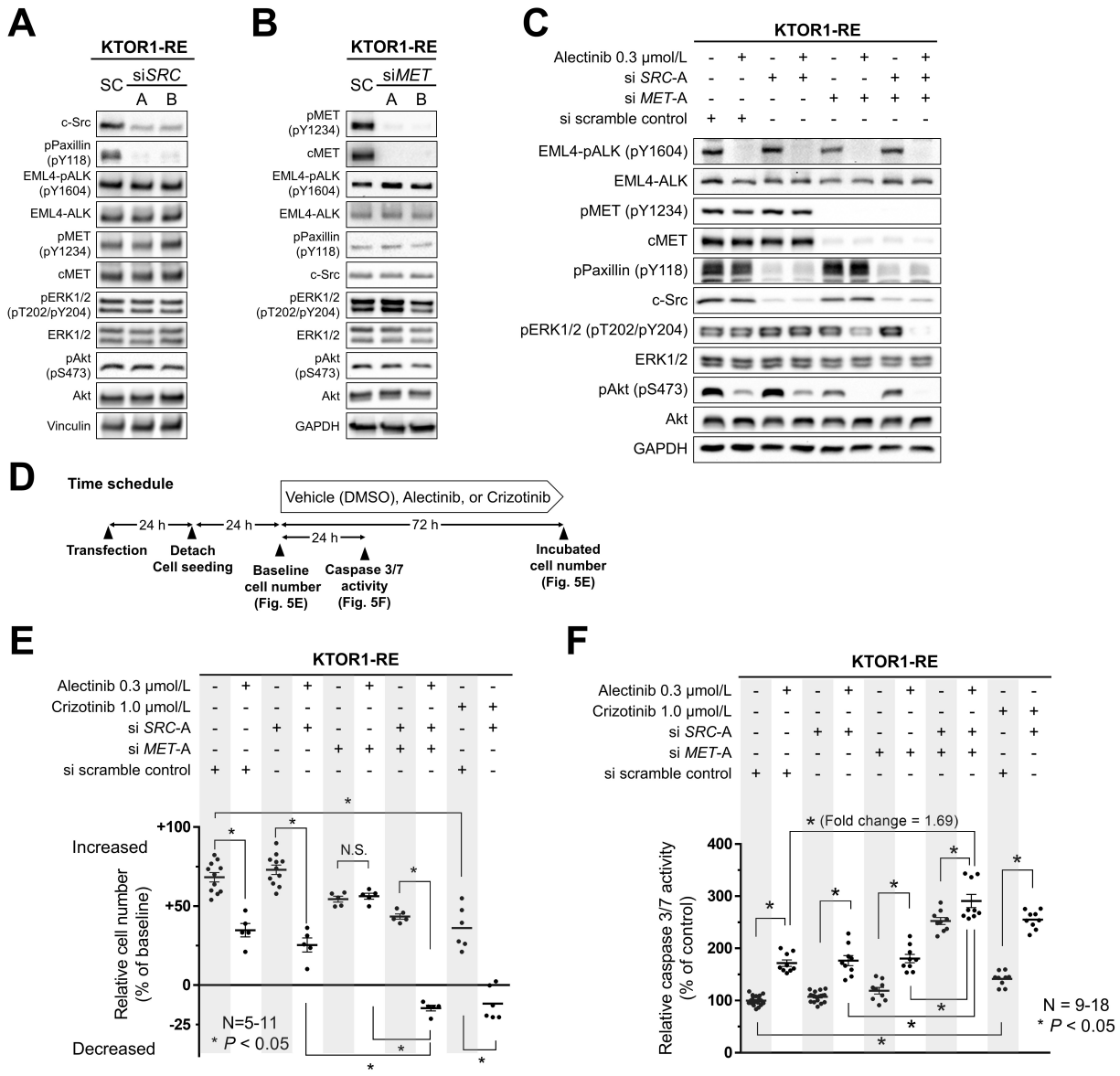

Fig. 5. Knockdown of *MET* and *SRC* overcame alectinib resistance

(**A, B**) The knockdown of *SRC* (**A**) or *MET* (**B**) using small interfering RNA (siRNA) was performed on KTOR1-RE. Cell lysate was obtained 72 h after transfection and analyzed by immunoblotting using the indicated antibodies. (**C**) The knockdown of *MET* and/or *SRC* was performed on KTOR1-RE. Sixty-six hours after transfection, cells were exposed to vehicle or 300 nM of alectinib for 6 h. Cell lysate was obtained and analyzed by immunoblotting using the indicated antibodies. (**D**) The time schedule for a cell growth or apoptosis assay performed on KTOR1-RE cells transfected with *SRC* and/or *MET* siRNA and subsequently treated with vehicle alectinib, or crizotinib. (**E**) A cell growth assay of KTOR1-RE. Cell numbers at baseline and after a 72-h incubation were quantified using CellTiter-Glo. The relative cell number was calculated with "(Value – Baseline value)/Baseline value". P-value was calculated using Mann-Whitney test. (**F**) Caspase 3/7 activity was quantified using Caspase-Glo after a 24-h treatment with alectinib or vehicle. P-value was calculated using Tukey test. The

result of replicate experiments of Fig. 5C, D, E, and F using another siRNA oligomer, si*SRC*-B and si*MET*-B, was presented in Fig. S5A-C.

Figure 6

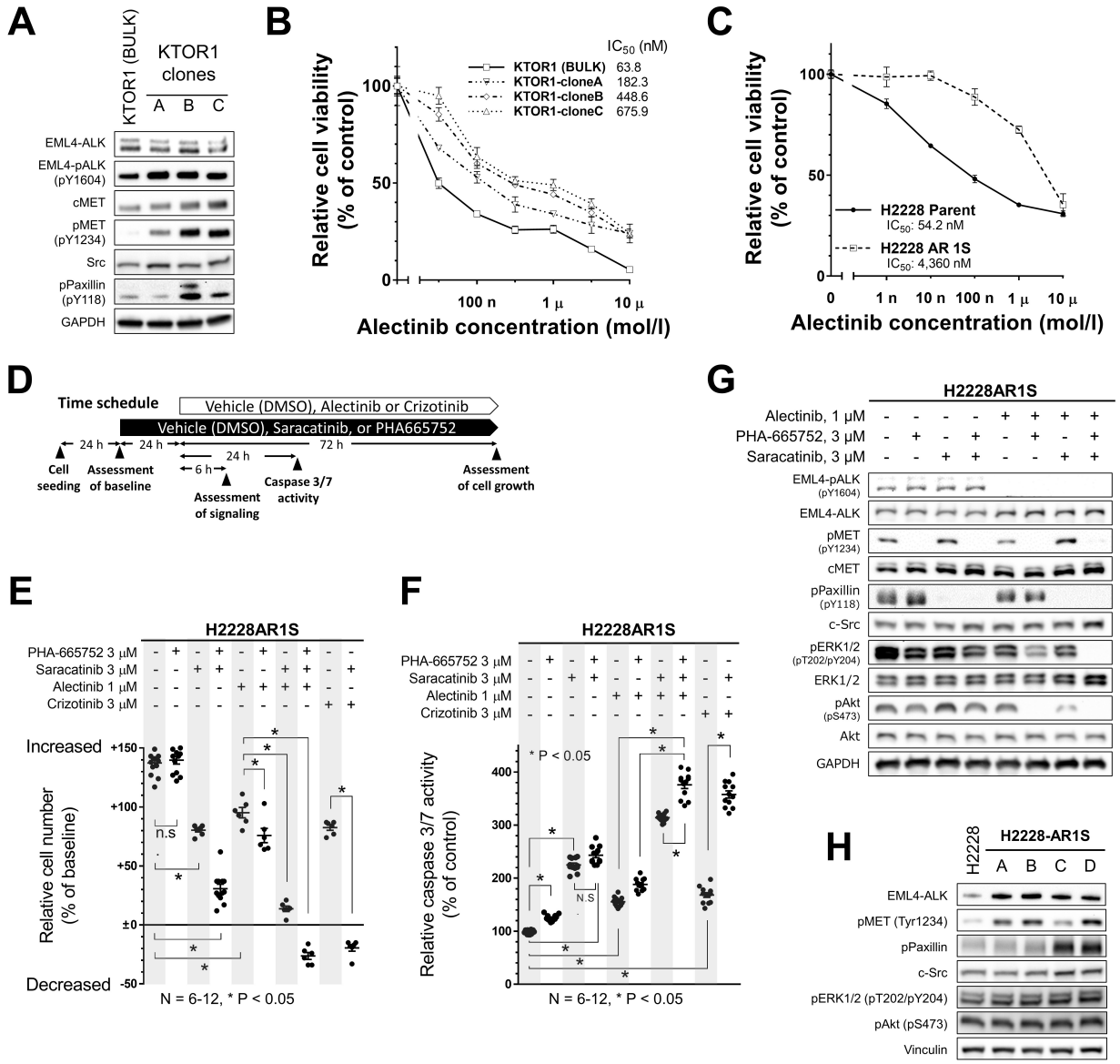

Fig. 6. KTOR1 cells and another alectinib-resistant cell line contained cells with Src and/or MET activity

(**A**) KTOR1 (BULK) cells and 3 clones (KTOR1-A, KTOR1-B, and KTOR1-C) established from KTOR1 cells were analyzed by immunoblotting using the indicated antibody. (**B**) KTOR1 (BULK) cells and the 3 clones (KTOR1-A, KTOR1-B, and KTOR1-C) established from KTOR1 cells were treated with the indicated concentrations of alectinib for 96 h (N=6). (**C**) H2228 cells and alectinib-resistant cells established from H2228 cells (H2228-AR1S) were treated with the indicated concentrations of alectinib for 72 h (N=6). (**D-G**) H2228-AR1S cells were treated with the indicated drugs. (**D**) The time schedule is shown. (**E**) A cell growth assay of H2228AR1S. Cell numbers at baseline and after treatment with indicated drugs were quantified using CellTiter-Glo. The relative cell number was calculated with "(Value – Baseline value)/Baseline value". P-value was calculated using Tukey test. (**F**) Caspase 3/7 activity was quantified using Caspase-Glo after a 24-h treatment with indicated drugs. All columns were compared and P-value was calculated using Tukey test. (**G**) A cell lysate

was obtained after a 6-h treatment with alectinib and analyzed by immunoblotting using the indicated antibody. (**H**) H2228 cells and 4 representative clones (H2228AR1S-A, B, C, and D) established from H2228-AR1S cells were analyzed by immunoblotting using the indicated antibody.

Figure 7

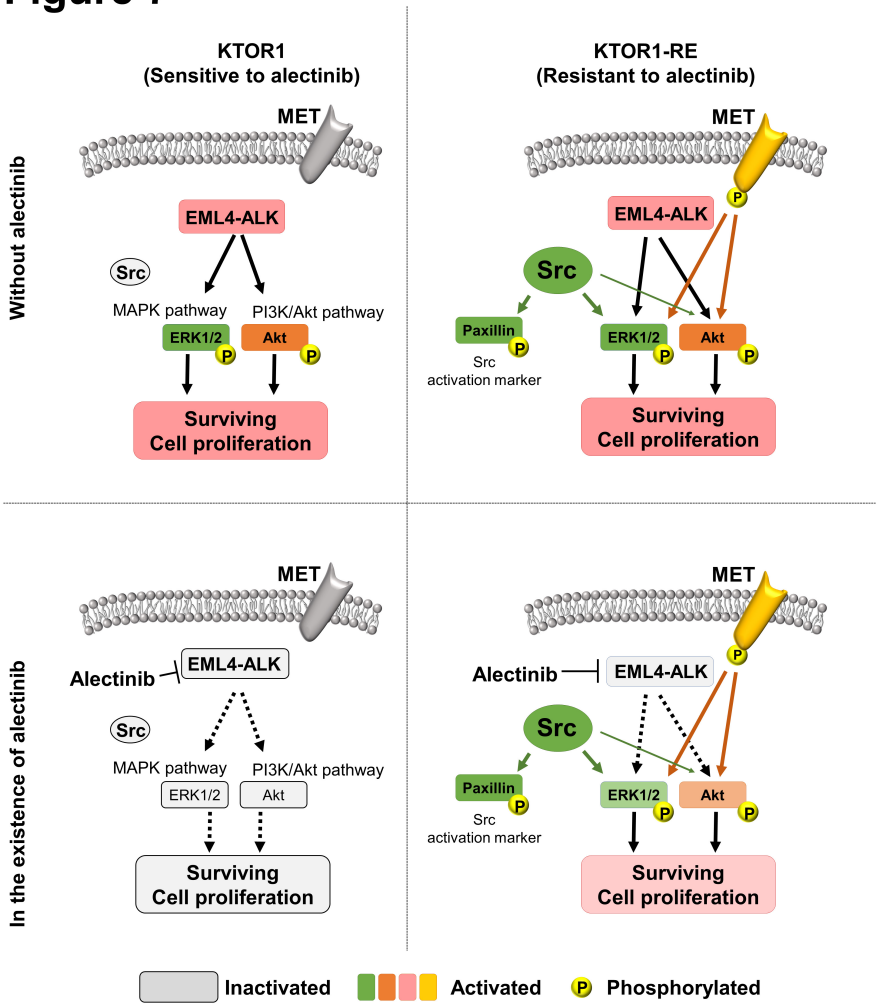

Fig. 7. Schematic explanation for the dual bypass signaling pathway of KTOR1-RE.

In KTOR1-RE cells, Src and MET maintained downstream survival, anti-apoptotic, and proliferation signaling (Akt and ERK1/2) independent of oncogenic EML4-ALK signaling. In the presence of alectinib, PI3K/Akt pathway was maintained by MET, and MAPK pathway was maintained Src and MET. KTOR1-RE cells survive and proliferate in the presence of alectinib because alectinib does not inhibit MET or Src.

Supplementary materials

Fig. S1. Supplementary data for Fig. 1

Fig. S2. Supplementary drug sensitivity data to ALK inhibitors in KTOR1 and KTOR1-RE.

Fig. S3. Supplementary results of the phosphoproteome analysis

Fig. S4. Saracatinib sensitized KTOR1-RE cells to crizotinib

Fig. S5. Combined knockdown of *MET* and *SRC* inhibited proliferation and induces apoptosis

Fig. S6. Supplementary data for Fig. 6

Table S1. Primer sequences for direct sequence of ALK exons

Table S2. Primer sequences for detection and sequence of *EML4-ALK* rearrangement

Table S3. Primer sequences for qRT-PCR

Data File S1. Data sets of the phosphoproteome analysis in KTOR1 and KTOR1-RE cells